18th IFHTSE CONGRESS
International Federation for Heat Treatment and Surface Engineering
IFHTSE
ANAIS
PROCEEDINGS
ISSN 1516-392X

FINITE ELEMENT ANALYSIS OF THE PHASE TRANSFORMATION DURING A HOT STAMPING PROCESS[1]

Philipp Olle[2]
Kathrin Voges-Schwieger[2]
Bernd-Arno Behrens[2]

Abstract
A technology to manufacture highest-strength automotive components is hot stamping. This process combines forming and heat treatment of sheet metal material. During and after the hot stamping process phase transformations from austenite to other phases occur. For a realistic prediction of the resulting component properties by means of Finite Element Analysis it is essential to consider the complex effects of phase transformation. Experimental and numerical investigations of hot stamping of a cap profile are carried out. In respect of the numerical investigations, aspects of a developed material model are presented, that considers the transformation-induced stresses and the plastic anisotropy. The model is tested by comparison of experiment and simulation with respect to phase fractions and distortion. Due to the temperature history during the forming phase and the heat treatment phase marginal distortion of the hot-stamped cap profile occurs. The microstructure is characterized by a phase mixture of martensite and bainite. The results of the numerical simulation correspond with those of the experimental investigations. A significant influence of transformation-induced stresses on the calculated part distortion is detected.
Key words: Hot stamping; Micro structural evolution; Numerical simulation; Plastic anisotropy.

[1] *Technical contribution to the 18th IFHTSE Congress - International Federation for Heat Treatment and Surface Engineering, 2010 July 26-30th, Rio de Janeiro, RJ, Brazil.*
[2] *Institute of Metal Forming and Metal-Forming Machines, Leibniz Universität Hannover, Germany.*

1 INTRODUCTION

A technology to manufacture highest-strength automotive components is hot stamping. This process combines the forming and heat treatment of a sheet metal material with the objective of hardening.[1] In general boron alloyed heat-treatable steels, e. g. 22MnB5 (1.5528), are used.

At the beginning of the process a blank or a preformed component of temperable steel is heated up to a temperature of about 950 °C to achieve austenitic microstructure. Afterwards it is formed with a cooled punch to quench the blank to get ultra high strength martensitic microstructure.

Currently this procedure is used by many automotive manufacturers to produce body structure components like crossbeams, side impact reinforcements, A- and B-pillars. In Figure 1 are given some examples for automotive parts of the VW Passat which are produced by hot stamping.

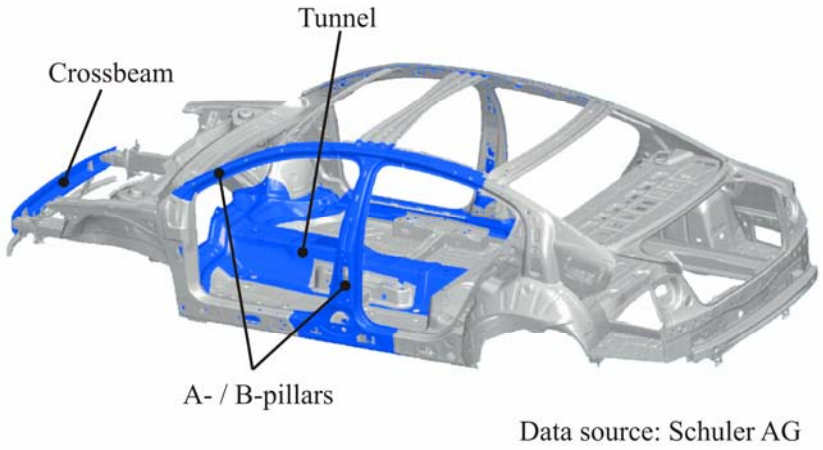

Figure 1. Application areas for hot-stamped components, using the VW Passat as an example.

During and after the hot stamping process phase transformations from austenite to other phases occur. For a realistic prediction of the resulting component properties by means of Finite Element Analysis it is essential to consider these complex effects of phase transformation. Commercial FE-systems which are adequate for simulation of hot stamping do not consider effects of phase transformation by default.

In literature several material laws for the consideration of phase transformation effects during hot stamping are presented.[2,3] In order to model the thermal-elastic-plastic-metallurgical behaviour the total strain increment:

$$d\varepsilon = d\varepsilon^{el} + d\varepsilon^{pl} + d\varepsilon^{th} + d\varepsilon^{tr} + d\varepsilon^{tp} \quad (1)$$

is described by the sum of the elastic (el), the plastic (pl), the thermal (th), the isotropic transformation (tr) and the transformation-induced plasticity (tp) strain increment. In these models the plastic behaviour is based on von Mises plasticity. But manganese-boron steels show a temperature and strain-rate dependent, anisotropic plastic behaviour (normal anisotropy).[4] The aim of this paper is to extend the material model of our previous work,[3] to take the normal plastic anisotropy of the material into account.

2 MATERIALS AND METHODS

2.1 Experimental Investigations

Within the framework of the experimental investigations hot-stamped cap profiles are manufactured and investigated with respect to distortion. Moreover the microstructure of the hot-stamped part is characterized by qualitative and quantitative metallography.

The hot stamping experiments are carried out on the hydraulic press Hydrap HPDZb 63 and by using a heatable tool system. To achieve high cooling rates a water cooling system is applied in the punch. The blank holder and the drawing die can be tempered by heating cartridges up to 300 °C. For the tool lubrication a graphite emulsion is used which is adequate for the occurring process temperatures.

The blanks are heated up to 950 °C in a furnace in five minutes. To avoid oxide scale blanks with a x-Tec coating are used. The unloading out of the furnace and the transport to the tools is done manually.

For hot stamping of the cap profiles the steel 22MnB5 (1.5528) with a thickness of 1.25 mm is used. The distance between the blank holder and the drawing die is set to 2.5 mm. The tool velocity is 27 mm/s and the blanks are drawn to a drawing depth of 65 mm. The hardening of the blanks takes a time of 60 s in the closed tools. The tool temperature is 20 °C. In Figure 2 a hot-stamped cap profile and the corresponding blank dimensions are shown.

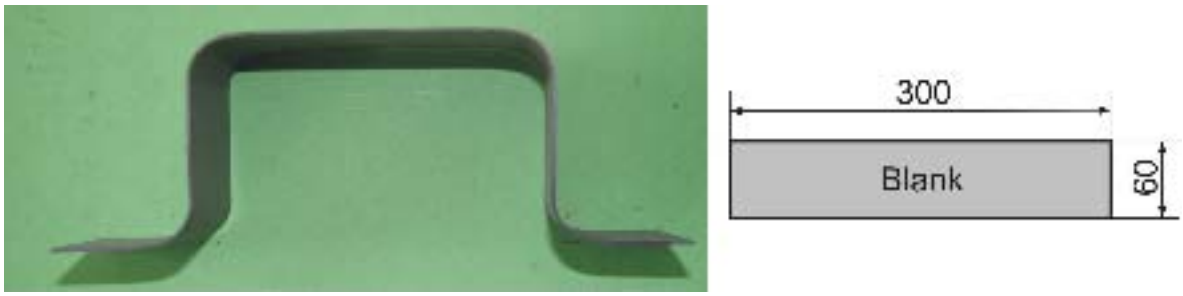

Figure 2. Hot-stamped cap profile and blank dimensions.

The geometry of the hot-stamped cap profiles is measured to investigate the distortion during the process. Moreover qualitative and quantitative metallographic investigations by light microscopy and by scanning electron microscopy (SEM) are carried out.

2.2 Material Model

For the simulation of the microstructure evolution the algorithm presented in our previous work,[5] is used. The algorithm needs the times of the beginning and the end of the phase transformation. These parameters can be taken from an isothermal time-temperature-transformation (ttt) diagram. Because the determination of this diagramm is a demanding task and there is no suitable data available from literature, in this paper a different approach is used.

To describe the mircostructure evolution the model of LI,[6] is extended. This model describes the diffusion-controlled phase transformation from austenite in ferrite, pearlite and bainite. To model the diffusionless phase transformation from austenite into martensite another approach is used.[5]

In LI's model the temperature dependent incubation times for the development of the product phases ferrite (F), pearlite (P) and bainite (B) are described by:

$$\tau_{\mathrm{F}}(\zeta_{\mathrm{F}},\vartheta)=\frac{f_{\mathrm{F}}}{2^{0.41G}\left(A_{\mathrm{e3}}-\vartheta\right)^{3}e^{-\frac{Q}{R(\vartheta+273°\mathrm{C})}}}S(\zeta_{\mathrm{F}})\ ,$$

$$\tau_{\mathrm{P}}(\zeta_{\mathrm{P}},\vartheta)=\frac{f_{\mathrm{P}}}{2^{0.32G}\left(A_{\mathrm{e1}}-\vartheta\right)^{3}e^{-\frac{Q}{R(\vartheta+273°\mathrm{C})}}}S(\zeta_{\mathrm{P}})\ \text{and} \qquad (2)$$

$$\tau_{\mathrm{B}}(\zeta_{\mathrm{B}},\vartheta)=\frac{f_{\mathrm{B}}}{2^{0.29G}\left(\vartheta_{\mathrm{Bs}}-\vartheta\right)^{2}e^{-\frac{Q}{R(\vartheta+273°\mathrm{C})}}}S_{\mathrm{B}}(\zeta_{\mathrm{B}})\ .$$

The incubation times describe the amount of time the phase transformation takes to reach a phase fraction ζ. The beginning and the end of a phase transformation are defined as the times when the phase fractions are ζ = 1 % respectively ζ = 99 %. The factors A_{e3}, A_{e1} and ϑ_{Bs} are the temperatures under which the associated phase transformation happens. Moreover the factor R is the universal gas constant and the factor G the grain size (ASTM number). The activation energy Q is Q = 6560 kJ/mol·K. The functions S and S_B are reaction rates. The factors f_F, f_P and f_B are functions of the chemical composition of the steel and are calculated by:

$$f_{\mathrm{F}}=\exp\left(1+6.31C+1.78Mn+0.31Si+1.12Ni+2.7Cr+4.06Mo+\boldsymbol{k_{\mathrm{BF}}B}\right),$$

$$f_{\mathrm{P}}=\exp\left(-4.25+4.12C+4.36Mn+0.44Si+1.71Ni+3.33Cr+5.19\sqrt{Mo}+\boldsymbol{k_{\mathrm{BP}}B}\right), \qquad (3)$$

$$f_{\mathrm{B}}=\exp\left(-10.23+10.18C+0.85Mn+0.55Ni+0.9Cr+0.36Mo+\boldsymbol{k_{\mathrm{BB1}}B}\right)\ .$$

The bold factors are the extension of LI's phase transformation model to take into account the influence of boron on the time-temperature-transformation behaviour. Moreover the reaction rates S and S_B have to be defined. The reaction rate S is:

$$S(\zeta)=\int_{0}^{\zeta}\frac{\mathrm{d}\zeta}{\zeta^{0.4(1-\zeta)}\left(1-\zeta\right)^{0.4\zeta}}\ . \qquad (4)$$

According to Kirkaldy,[7] the reaction rate for the bainitic phase transformation is defined as:

$$S_{\mathrm{B}}(\zeta_{\mathrm{B}})=S(\zeta_{\mathrm{B}})\exp\left(\zeta_{\mathrm{B}}^{2}\left(1.9C+2.5Mn+0.9Ni+1.7Cr+4Mo+\boldsymbol{k_{\mathrm{BB2}}B}-2.6\right)\right)\ . \qquad (5)$$

The bold factor is also an extension of the phase transformation model to take into account the influence of boron.

The factors k_{Bf}, k_{BP}, k_{BB1} and k_{BB2} are determined by numerical identification. A least squares method is used. For this the phase transformation algorithm is applied to simulate the cooling curves from the continouus time-temperature-transformation (cct) diagram taken from literature.[8] The calculated and measured points of the beginning and the end of the phase transformations and the calculated and measured phase fractions are taken in the least squares method into account.

In the following the material model presented in our previous work,[3] is extended to anisotropic plasticity. For this the Hill yield criterion,[9] is used. Because the plastic model only affects the deviatoric stress tensor it is shown in the following passage how to model this part. The modelling of the hydrostatic part of the stress tensor is exactly the same as in the mentioned literature. In tensor notation the Hill yield criterion can be described by the equation:

$$F_{\mathrm{H}} = \sqrt{\boldsymbol{s} \cdot \boldsymbol{H}\boldsymbol{s}} - k_{\mathrm{f}} \leq 0 \quad . \tag{6}$$

Here the variable $\boldsymbol{s}$ is the deviatoric stress tensor and the variable k_{f} the yield stress of the material. The variable $\boldsymbol{H}$ the Hill anisotropy tensor (fourth order tensor) which is defined in matrix notation by:

$$[\boldsymbol{H}] = \begin{bmatrix} 1 & -\frac{r}{1+r} & -\frac{r}{1+r} & 0 & 0 & 0 \\ -\frac{r}{1+r} & 1 & -\frac{1}{1+r} & 0 & 0 & 0 \\ -\frac{r}{1+r} & -\frac{1}{1+r} & \frac{2}{1+r} & 0 & 0 & 0 \\ 0 & 0 & 0 & 2\frac{1+2r}{1+r} & 0 & 0 \\ 0 & 0 & 0 & 0 & 2\frac{1+2r}{1+r} & 0 \\ 0 & 0 & 0 & 0 & 0 & 2\frac{1+2r}{1+r} \end{bmatrix} \tag{7}$$

with the normal anisotropy r that is temperature and strain rate dependent. According to LECHLER,[4] in this paper the normal anisotropy is calculated by:

$$r = r_{\mathrm{i}} e^{\left(-c_r(\vartheta_i - \vartheta) - c_\varphi \dot{\varphi}\right)} \quad . \tag{8}$$

Here the variables r_{i}, c_{r}, ϑ_{i} and c_{φ} are material parameters and the variable ϑ is the temperature and the factor $\dot{\varphi}$ the plastic strain rate.

In case of the Hill yield criterion the plastic strain increment in equation 1 can be determined by

$$\mathrm{d}\boldsymbol{\varepsilon}^{\mathrm{pl}} = \frac{\mathrm{d}\tilde{\varepsilon}^{\mathrm{pl}}}{k_{\mathrm{f}}} \boldsymbol{H}\boldsymbol{s}_1 \quad . \tag{9}$$

Here the variable $\mathrm{d}\tilde{\varepsilon}^{\mathrm{pl}}$ is the equivalent plastic strain increment and $\boldsymbol{s}_1$ the deviatoric stress tensor at the end of the time step.

Leblond's model for the transformation induced plasticity is modified to take into account the Hill anisotropy. It is described by:

$$\mathrm{d}\boldsymbol{\varepsilon}^{\mathrm{tp}} = -\frac{3}{2}\sum_{k=1}^{4} 2\left(\frac{\mathrm{d}V}{V}\right)_{\mathrm{A},k} h\left(\frac{\sigma_{\mathrm{H}}}{k_{\mathrm{f}}}\right) d\zeta_k \ln(\zeta_k)\frac{\boldsymbol{s}_1}{k_{\mathrm{f}}^{\mathrm{A}}} = \frac{3}{2}\mathrm{d}\tilde{\varepsilon}^{\mathrm{tp}}\frac{\boldsymbol{s}_1}{k_{\mathrm{f}}^{\mathrm{A}}} \quad . \tag{10}$$

The phase fraction of the product phase k is represented by ζ_k (k = 1: ferrite, k = 2: pearlite, k = 3: bainite, k = 4: martensite). Furthermore, the yield stress of austenite is $k_{\mathrm{f}}^{\mathrm{A}}$ and the equivalent stress according to Hill is σ_{H}. The factor $(\mathrm{d}V/V)_{\mathrm{A},k}$ describes the volume change due to a phase transformation from austenite to the product phase k. Because in the used microstructure evolution algorithm more than one new phase can occour within one time step, the summation is done over all product phases k. The correction function h is defined according to Leblond.[10]

After some mathematical conversions the deviatoric stress tensor $\boldsymbol{s}_1$ at the end of the time step can be calculated by:

$$\boldsymbol{s}_1 = \left(\left(1 + c_1^{\mathrm{tp}}\right)\overset{4}{\boldsymbol{I}} + c_1^{\mathrm{pl}}\boldsymbol{H}\right)^{-1}\boldsymbol{s}_{\mathrm{tr,el}} \quad . \tag{11}$$

The factors $c_1^{\mathrm{tp}}, c_1^{\mathrm{pl}}$ are defined as $c_1^{\mathrm{tp}} = 3G\,\mathrm{d}\tilde{\varepsilon}^{\mathrm{tp}}/k_{\mathrm{f}}^{\mathrm{A}}$ and $c_1^{\mathrm{pl}} = 2G\,\mathrm{d}\tilde{\varepsilon}^{\mathrm{pl}}/k_{\mathrm{f}}$. The factor $\overset{4}{\boldsymbol{I}}$ is the fourth order unity tensor and the variable G is the shear modulus. Moreover the elastic trial stress $\boldsymbol{s}_{\mathrm{tr,el}}$ can be calculated by $\boldsymbol{s}_{\mathrm{tr,el}} = \boldsymbol{s}_0 + 2G\mathrm{d}\boldsymbol{\varepsilon}^{\mathrm{D}}$ from the deviatoric stress tensor $\boldsymbol{s}_0$ at the beginning of the time step and the deviatoric strain increment $\mathrm{d}\boldsymbol{\varepsilon}^{\mathrm{D}}$. By these modifications the transformation-induced stresses and the plastic anisotropy are considered simultaneously in one material model for the first time.

2.3 FE-Model

The used Fe-model of the process for hot stamping the cap profile is shown in Figure 3. Because of symmetries to the x-z plane and the y-z plane only a quarter of the real process is calculated. The tools are modelled as solids and a contact dependent heat transfer coefficient is considered.

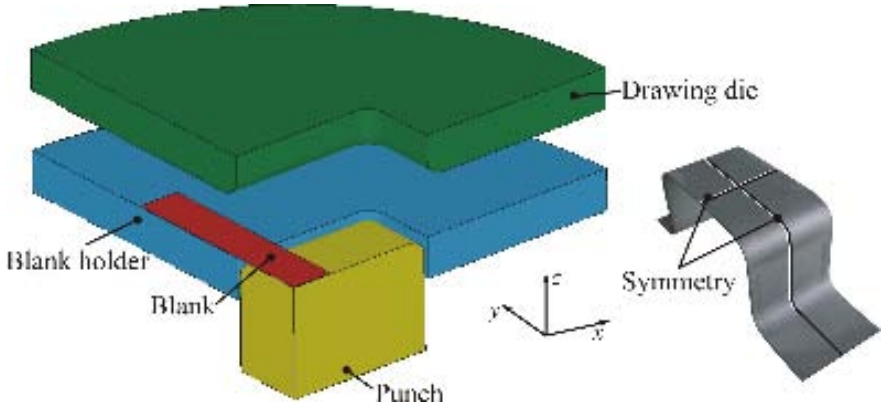

Figure 3. FE-model of the hot stamping process for forming a cap profile.

3 RESULTS AND DISCUSSION

3.1 Results of the Experimental Investigations

In Figure 4 the measured outline contour of the cap profile is compared with the desired geometry. As it can be seen, only marginal distortion occurs. Notable is the undercut in the edge. This undercut is caused by the transformation-induced stresses during the heat treatment phase.

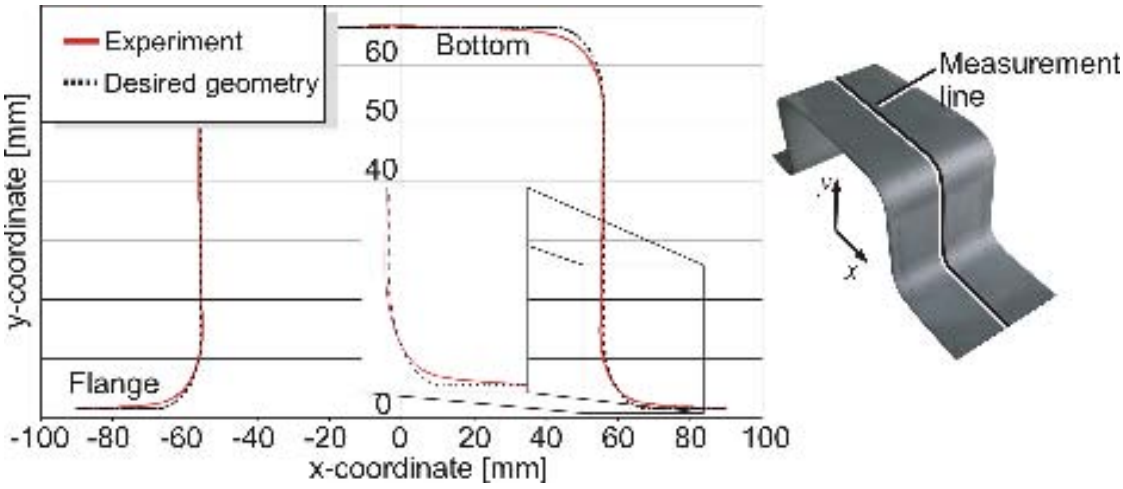

Figure 4. Distortion of the hot-stamped cap profile.

Moreover metallographic investigations are carried out. One important parameter in the microstructure evolution model is the austenite grain size. The averaged grain diameter after a heating on 950 °C in five minutes is between 35 µm and 50 µm. This corresponds to a grain size G of $6 < G < 7$ (ASTM-number).

The microstructure in the hot-stamped cap profiles is investigated with respect to the occurring phase fractions. As it is shown in Figure 5 the phase fractions are determined at six measuring points in the middle of the cap profile. In the flange (MP 6) only martensite occurs due to the high cooling rates which are caused by the two-sided tool contact.

At the measuring points MP 3 to MP 5 bainite fractions up to $\zeta_B = 11$ % are existent. In these areas the cooling velocities are lower than in the flange. Moreover the plastic deformation affects the critical cooling velocity in these part areas. The highest bainite fractions are in the bottom of the cap profile. Here the slowest cooling velocities occur and so bainite fractions up to $\zeta_B = 57$ % are existent.

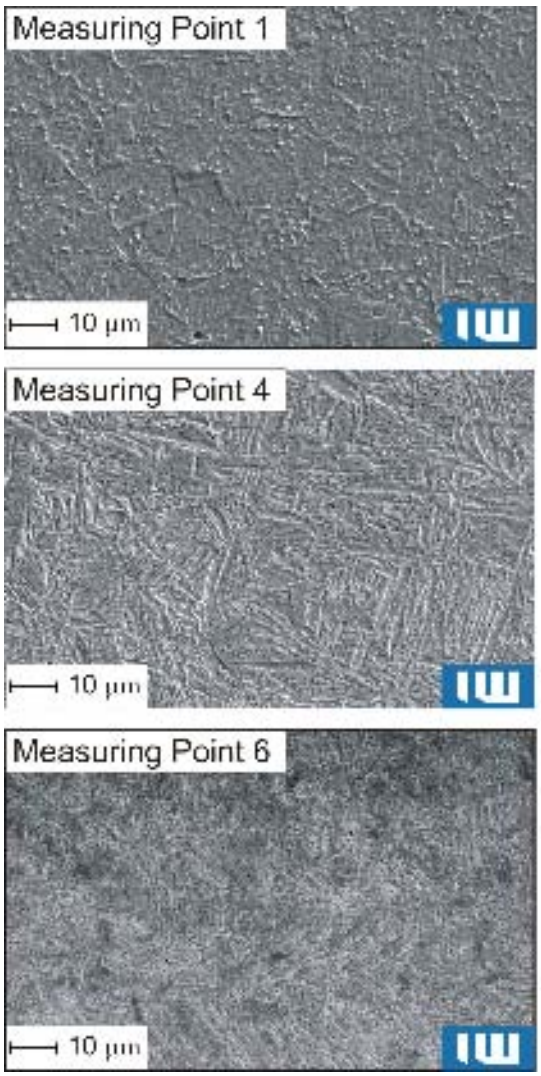

Measuring Point [-]	Bainite ζ_B [%]	Martensite ζ_M [%]
1	57	43
2	24	76
3	4	96
4	11	89
5	5	95
6	0	100

Figure 5. Microstructure Distribution.

3.2 Results of the Numerical Investigations

The parameters for the phase transformation model are determined by numerical identification. The determined parameters are k_{Bf} = 549 k_{BP} = 270, k_{BB1} = 297 and k_{BB2} = 1127. As Figure 6 shows with this parameter set the calculated and measured lines for the beginning and the end of the phase transformations agree. Especially the beginning and the end of the phase transformations from austenite into bainite and pearlite are mapped very well.

It is obvious that the determined parameter set is not applicable to arbitrary manganese boron steels. For that it is necessary to investigate many material compositions with different chemical compositions. But for the investigations at the steel 22MnB5 in this paper it is possible to use this parameter set.

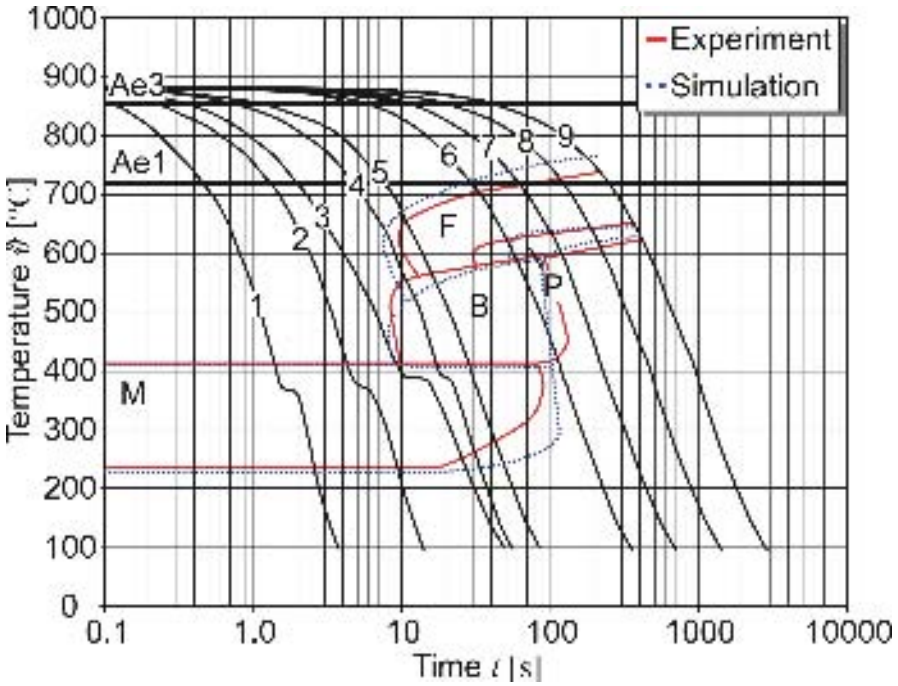

Figure 6. Comparison of experimental and calculated cct-diagram.

The simulated microstructure distribution in the cap profile is shown in Figure 7. Due to the temperature and forming history only martensite and bainite occurs in the cap profile. Thereby a martensite content up to ζ_M= 100 % occurs what is in general the aim in hot stamping.

The calculated values agree with the experimental data very well. The small deviations can be partly explained by the complex contact conditions which significantly affect the temperature history and can not be modeled exactly.

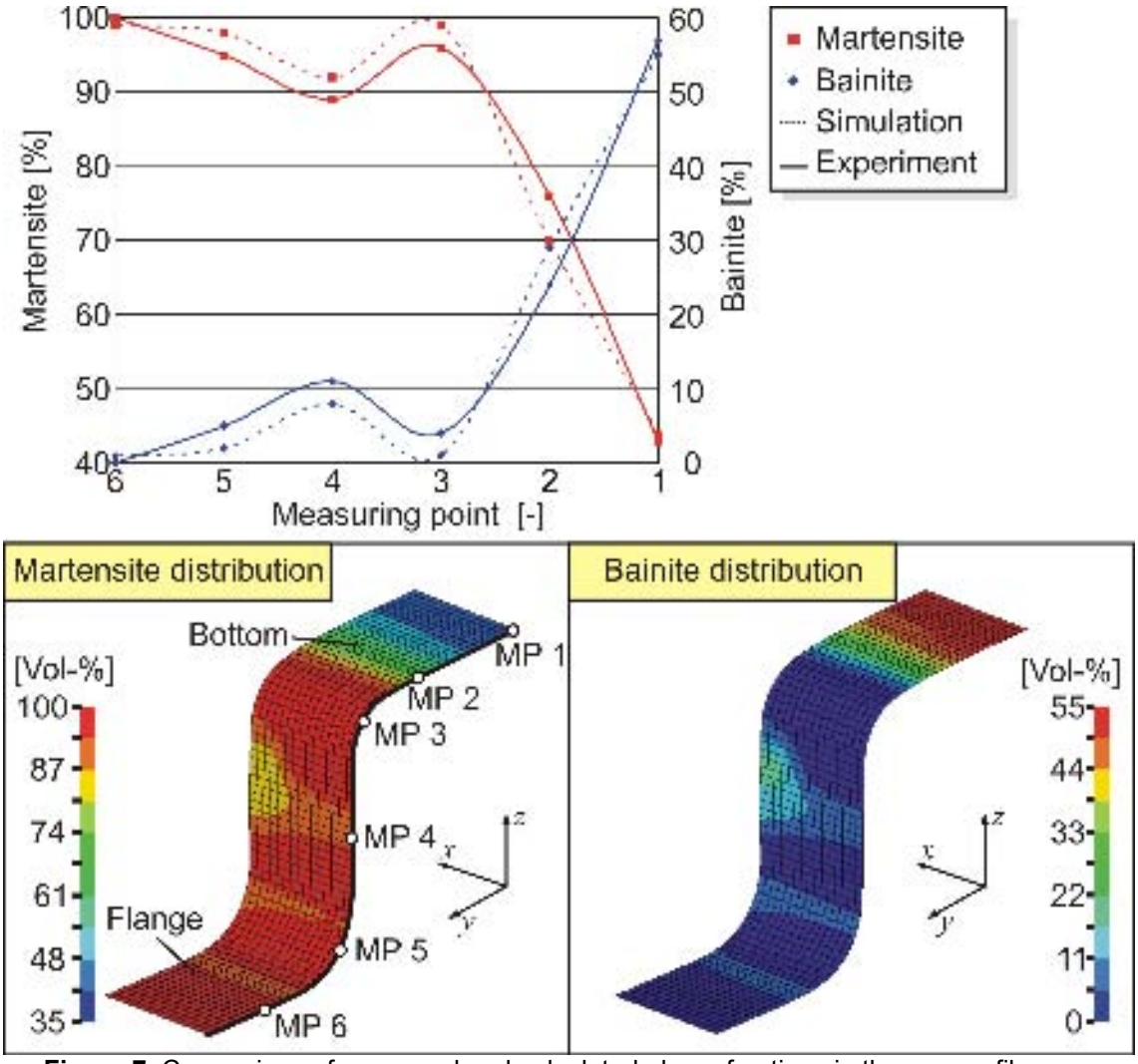

Figure 7. Comparison of measured and calculated phase fractions in the cap profile.

Moreover with the FE-model three simulations are performed. In the first simulation the effects of phase transformation on the mechanical behaviour are neglected. In the second simulation the isotropic transformation strains are considered and in the third also the transformation-induced plasticity strains are taken into account. The measured and calculated contours of the final geometry are drawn in Figure 8.

As one can see the phase transformation has a significant influence on the distortion behaviour of the cap profile. By considering the phase transformation much less distortion occurs than in the case with neglected phase transformation. Especially in the flange the distortion is reduced. A comparison with the experimental results shows that the simulated contour matches the experimental contour better when phase transformation is considered.

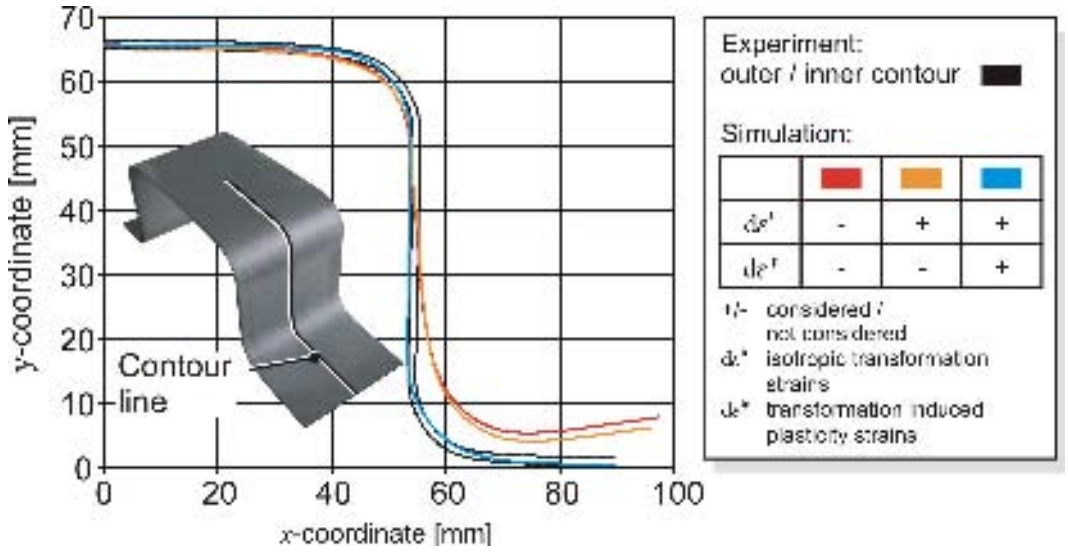

Figure 8. Influence of phase transformation on the calculated part contour.

4 CONCLUSIONS

For a realistic prediction of final component properties, for instance residual stresses and distortion, it is essential to consider the complex effects of phase transformation in the simulation of hot stamping. The extended material model which takes into account transformation-induced stresses and the plastic anisotropy simultaneously was used to simulate the hot stamping processes. As the results show the calculated phase fractions agree with those of the experimental data. The numerical simulations show that the phase transformation has significant effects on the distortion behaviour. To get realistic results by simulation of hot stamping processes it is essential to consider the effects of phase transformation in process simulation.

Acknowledgement

The authors gratefully acknowledge the financial support of the German Research Foundation (DFG) for this research work by grant BE 1691/11-2. Also thanks to the Institute of Materials Science of the Leibniz Universität Hannover for the metallographic investigations.

REFERENCES

1 LENZE, F.-J.; HELLER, T.; SIKORA, S. Herstellung von Karosseriebauteilen aus warmumgeformten höchstfesten Stahlwerkstoffen. In: EFB-KOLLOQUIUM: „Multifunktionale Bauteile und Verfahren zur Erhöhung der Wertschöpfung in der Blechbearbeitung“, Fellbach, Germany, Febuary 15-16, 2005.

2 ÅKERSTRÖM, P. Modelling and Simulation of Hot Stamping. *Luleå University of Technology (Sweden), PhD thesis,* 2006.

3 BEHRENS, B.-A.; OLLE, P. Consideration of Transformation-Induced Stresses in Numerical Simulation of Press Hardening. In: PLASTICITY CONFERENCE, Kailua-Kona, 03.-08.01.08.

4 LECHLER, J. Grundlegende Untersuchungen zur Beschreibung und Modellierung des Werkstoffverhaltens von presshärtbaren Bor-Manganstählen. *Friedrich-Alexander Universität Erlangen-Nürnberg, PhD thesis,* 2008.

5 BEHRENS, B.-A.; OLLE, P. Consideration of Phase Transformations in Numerical Simulation of Press Hardening. *steel research, 78, No. 10-11, pp. 784-790,* 2007.

6 LI, M. V. ; NIEBUHR, D. V. ; MEEKISHO, L. L. ; ATTERIDGE, D. G. A computational model for the prediction of steel hardenability. *Metallurgical and Materials Transactions B,* n. 3, p. 661–672, 1998.

7 KIRKALDY, J. S. ; VENUGOPALAN, D. Prediction of Microstructure and Hardenability in Low Alloy Steels. In: Phase Transformation in Ferrous Alloy. Philadelphia, Pennsylvania: The Metallurgical Society of AIME, 1983.

8 NADERI, M. Hot Stamping of Ultra High Strength Steels. *Rheinisch-Westfälische Technische Hochschule Aachen*, PhD thesis, 2007.

9 HILL, R. A theory of the yielding and plastic flow of anisotropic metals. *Proceedings of the Royal Society. London,193, pp. 281-297*, 1948.

10 LEBLOND, J. B. Mathematical modelling of transformation plasticity in steels II: coupling with strain hardening. In: *International Journal of Plasticity* 5, p. 573-591, 1989.